31506

Approved for public release;
distribution unlimited.

Low-Resistance, High-Power-Efficiency Vertical Cavity Microlasers

Sponsored by
Advanced Research Projects Agency
ARPA Order No. 8678
Monitored by AFOSR Under Contract No. F49620-92-C-0053

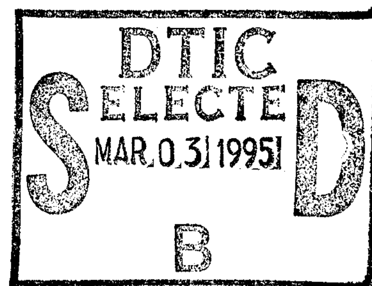

Annual Technical Report
14 September 1993

(1) ARPA Order 8678
(2) Program Code 2D10
(3) Photonics Research Incorporated
(4) Effective Date: 15 August 1992
(5) Expiration Date: 14 November 1994
(6) Contract Dollars: $452,522
(7) Contract No. F49620-92-C-0053
(8) P.I.: Dr. Jack L. Jewell
Phone: (303) 678-5225 ext. 15
(9) Program Mgr.: Dr. Alan Craig
Phone: (202) 767-4931
(10) High-Efficiency Microlasers

19950224 031

The views and conclusions contained in this document are those of the authors and should not be interpreted as necessarily representing the official policies or endorsements, either expressed or implied, of the Advanced Research Projects Agency or the U.S. Government.

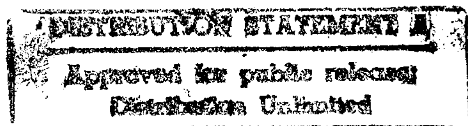

DTIC QUALITY INSPECTED 1

94 5 31 144

Low-Resistance, High-Power-Efficiency Vertical Cavity Microlasers

Annual Technical Report

1. Report Summary

Introduction

The purpose of this project is to improve the most critical "bottom-line" characteristic of vertical-cavity microlasers, namely total power efficiency. This improvement will enable the commercialization of large arrays of semiconductor lasers integrated on single chips. Vertical-cavity surface-emitting lasers (VCSELs, tradenamed LASE-ARRAY™ by Photonics Research Incorporated) are tiny semiconductor lasers, typically about 10 μm in diameter, whose optical cavities and electrical injection schemes are radically different from conventional "edge-emitting" semiconductor lasers. The VCSEL geometry emits high-quality beams perpendicular to the face of the chip, rather than out the edge of the chip, and can be readily fabricated in one- and two-dimensional arrays. VCSELs have many other advantages over edge-emitters. Overview articles of VCSEL properties can be found, for example, in Jewell, 1991a, 1991b, 1992a, 1992b.

Central to the attainment of high power efficiency (wallplug efficiency) is the simultaneous minimization of: 1) electrical resistance, 2) optical absorption in the cavity, and 3) threshold current. Most approaches to improving one of these characteristics does so only at the expense of another. For example, decreasing the resistance by increasing the doping levels in the semiconductors will simultaneously increase the optical absorption. The basis of this project is to develop VCSEL designs which circumvent the "resistance-absorption tradeoff." The most elegant design approach and the one which promises the highest efficiency modulates the doping concentrations, making it higher in regions where the standing-wave optical intensity is low and lower throughout the rest of the structure. This approach was outlined in the proposal. Another feature required for high efficiency is confinement of current to the central portion of the VCSEL, where optical intensity is highest.

Results

Soon after submission of the proposal, a preliminary demonstration of the modulation-doped approach was made through a collaboration between PRI and Bellcore. The result was a record-low threshold voltage of 1.7 volts for VCSELs [Jewell, 1992a; Scherer, 1992]. Previously, VCSELs required a minimum of about 2.5 volts for threshold. The significance of this difference is better appreciated by comparing these voltages to the bandgap energy of the active material, about 1.45 volts, below which essentially no current flows. The "additional" voltages required above bandgap are then 0.25 volts for the new devices compared to greater than 1 volt in previous devices. The results validated our proposed approach to fabricating low-resistance VCSELs. The specific resistance (resistance x area) was nearly as low as in highly-developed edge-emitters. High power efficiency was not achieved, largely due to limitations in available photolithographic mask patterns which in turn limited the sophistication of the fabrication process.

Within the contract period, we demonstrated an 8x8 array of quasi-visible, 725-nm-emitting VCSELs which used the proposed approach. A color photograph of the LASE-ARRAY™, which appeared in Photonics Spectra, is presented in this report (Fig. 1). A process follower was developed for the manufacture of high-efficiency VCSELs. Photolithographic masks to accomplish the fabrication process were laid out and fabricated. More detailed calculations have been carried out to predict and optimize the performances of VCSELs. The calculations include recently-reported improvements in p-type mirror design and improvements made to the design of the bottom, n-doped side of the VCSEL. Our experimental results and calculations conclude that the wallplug efficiencies in VCSELs can approach the high levels of 40-50 % attained in edge-emitters.

A bullet list of the accomplishments thus far within the contract period is presented in chronological order as follows:

- Calculated optical and electrical characteristics of modulation-doped VCSEL structures for maximum doping levels of $\leq 10^{19}$ cm^{-3} as limited by beryllium as the dopant. Selected an 8-layer structure as optimal for the constraint on concentration.
- Purchased DW-2000 software package for the layout of photolithographic masks.
- Designed "stratified-p-layer" vertical-cavity lasers for emission at 740, 850 and 980 nm with doping concentrations $\leq 10^{19}$ cm^{-3} as limited by beryllium as the dopant.
- Developed process follower for the fabrication of vertical-cavity lasers having shallow implantation depths and dielectric mirrors.
- Designed full set of masks according to the process follower and had the masks fabricated.
- Demonstrated 8x8 array of 725 nm vertical-cavity lasers (Photonics Spectra, Nov. '92 issue, p.126).
- Filed U.S. Patent Application serial number 07/978,391 "Optical Beam Delivery System," filing date 18 November 1992.
- Filed U.S. Patent Application serial number 07/994,976 "Vertical Cavity Surface-Emitting Laser with Expanded Cavity," filing date 22 December 1992.
- Designed new "hybrid mirror" lasers, whose top mirror is partially semiconductor and partly dielectric, for 780 nm and 850 nm emission.
- Had a hybrid mirror wafer grown. Tested the wafer through reflectance and photoluminescense spectra, which verified the growth quality.
- Evaluated potential performance of VCSELs using recently published low-resistance p-mirrors.
- Deposited dielectric mirrors on test wafers in preparation for process development.

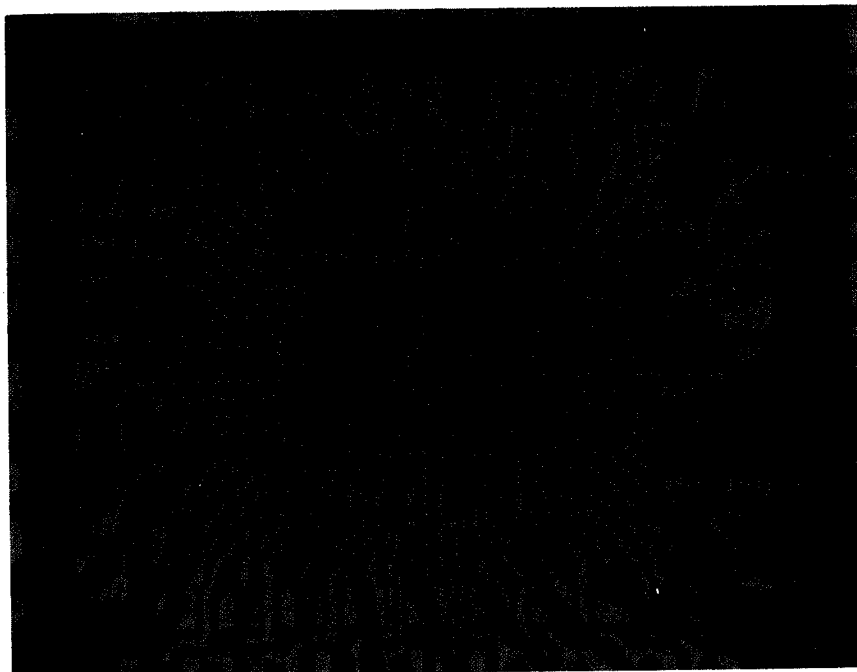

Fig. 1. Photomicrograph of a partially-activated 8x8 LASE-ARRAY™ emitting at 725 nm.

Accession For
NTIS GRA&I ☑
DTIC TAB ☐
Unannounced ☐
Justification
By
Distribution/
Availability Codes
Dist | Avail and/or Special
A-1

2. VCSEL Design Approaches

Background

The VCSEL is a complex 3-dimensional structure whose optical requirements and electrical pumping geometry are very different from any previous electronic or optoelectronic device. For this reason, early VCSEL demonstrations involved simple designs and did not achieve high efficiency. The 40-50 % wallplug efficiencies in edge-emitters was achieved through many years of development, initially involving qualitative structural design changes and followed by quantitative refinements. VCSELs are in the qualitative improvement phase. One requirement for high efficiency, low threshold current density, was achieved in VCSELs several years ago by fabricating cavities with high enough finesse to work with a few quantum wells or even a single quantum well [Jewell, 1989; Lee, 1989]. The lowest threshold VCSELs used single quantum wells (SQW) [Geels, 1990], but had very low output power and efficiency. The low efficiency resulted from optical absorption in the doped semiconductor mirrors and from high electrical resistance. A SQW VCSEL offers the best chance for achieving high efficiency and it is most sensitive to optical absorption.

Modulation-Doped Design

We have designed modulation-doped VCSELs for emission at 740 nm, 850 nm and 980 nm. A wafer was grown and fabricated which showed lasing at 725 nm. More details on the results will be presented in Section 4.

In the modulation-doped VCSEL described in the proposal the current completely bypasses the top mirror through conductive layers which contribute negligibly to the reflectivity. It can be considered an extreme departure from the conventional design where current flows completely through the top mirror. Both designs are illustrated in Figure 2. The modulation-doped design thus bypasses the potential barrier structure inherent to the interfaces of a semiconductor mirror which causes the high resistance. The sheet resistance of the conductive layer must be sufficiently low that the transverse current flow (Fig. 2b) does not have high resistance. For conventional doping levels, on the order of 10^{19} cm^{-3} or less, the conductive layer must be about 1 µm thick. A 1-µm-thick layer comprises about 8 half-wave periods of the modulation-doped structure. An optimized modulation-doped layer confines the high doping concentrations to regions in the minima of the standing wave intensity pattern. To aid in this confinement, our designs use a lower bandgap material in these regions, for example AlGaAs of a lower Al composition.

The top contact surface of the modulation-doped conductive layer can be designed to be either in a peak or in a trough of the standing waves. Either placement involves tradeoffs relating to the fact that the top surface forms the electrical contact. High doping is appropriate for the electrical contact, but it causes high absorption in the peak of the standing wave. Thus electrical contacting considerations favor placement of the top surface in the trough. However this has two optically-related disadvantages. First, more layers are required for the dielectric mirror due to the fact that the dielectrics must start with a high-index layer rather than low-index. This relation between the dielectric layers and the standing wave position is fundamental to the operation of thin film cavities. Second, it is more difficult to derive information about the thickness of the optical cavity. In the case where a peak of the standing waves occurs at the top surface, a weak cavity resonance occurs at the desired lasing wavelength, which is in the center of the reflectivity region of the mirrors. Departure of the resonance from the desired wavelength indicates an error in the thickness of the conductive layer which can be corrected for in the deposition of the dielectric mirrors (as demonstrated [Scherer, 1992]). When the top surface is in a trough of the standing waves, the lasing wavelength lies directly between cavity resonances, making it difficult to determine the optical thickness of the conductive layer. It is possible to bypass this tradeoff through shallow etching or diffusion. The epitaxial structure would be grown fully optimally for the optical characteristics, with low doping and the standing wave peak at the top surface. In fabrication, a shallow etch of about 600 Å would reach the high-doped layer suitable for electrical contacting <u>outside</u> the optical cavity region. In this way, both optical and electrical characteristics are optimum. The shallow etch could also be replaced by a shallow diffusion of appropriate p-type dopant, e.g. zinc.

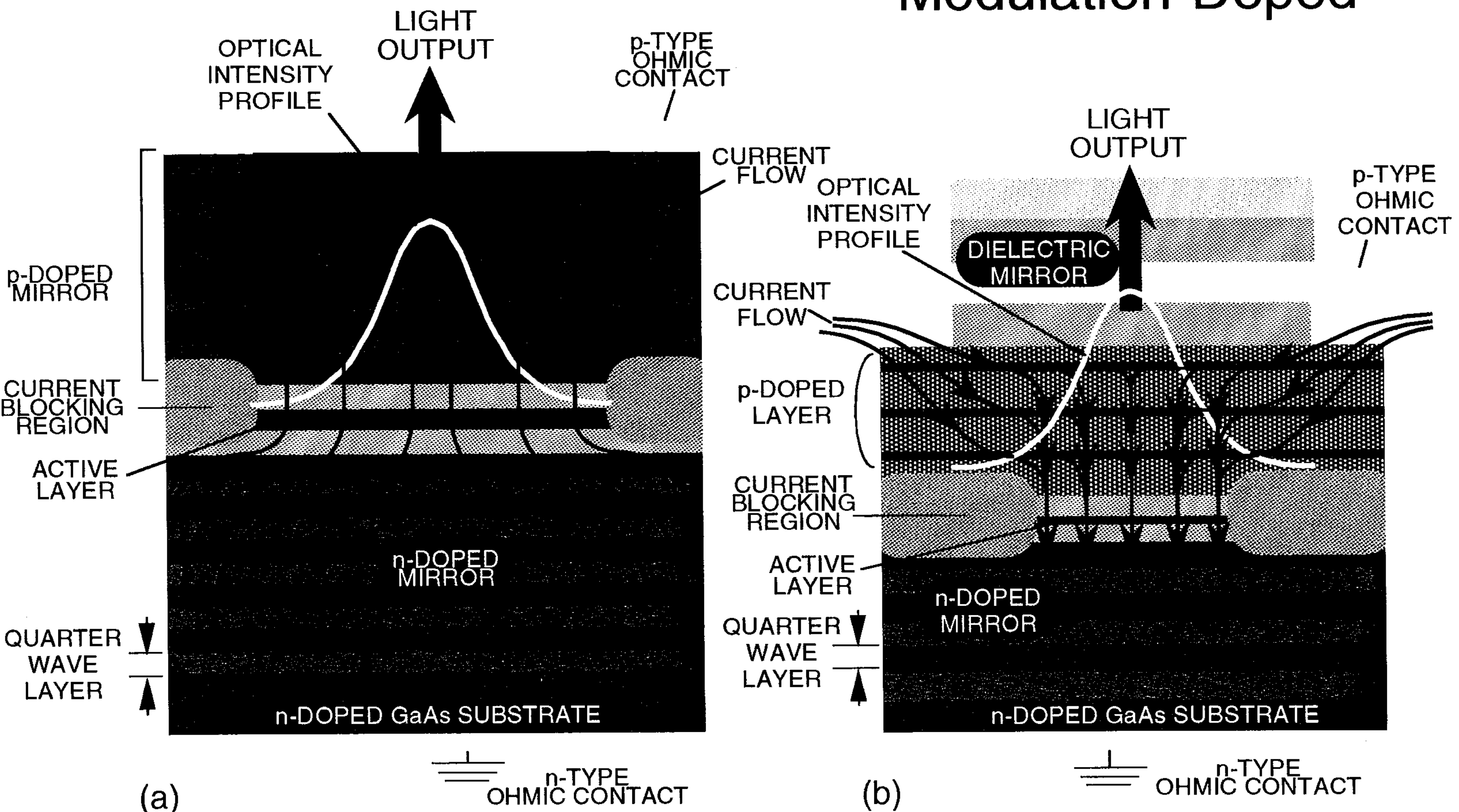

Figure 2. Comparison of electrical pumping geometries between (a) "conventional" and (b) modulation-doped VCSEL designs.

Hybrid-Mirror Design

For moderate doping levels of 10^{19} cm^{-3} or less, the ~1 μm of material required for low transverse resistance is sufficiently thick that significant reflectivity may be obtained from it. We have designed "hybrid-mirror" VCSELs for 780-nm, 850-nm, and 980-nm emission. Although the hybrid mirror VCSELs are not expected to have resistance/absorption losses as low as the modulation-doped VCSELs, the fabrication should be simpler owing to the greater precision in testing the epitaxial structure and the fewer required dielectric mirror layers. Furthermore the losses might eventually reach levels sufficiently low to be negligible anyway. Since the epitaxial portion of the hybrid mirror does not need to produce high reflectivity, its structure can be designed to accommodate current flow. For example, the component materials of the material can have less than 50% difference in aluminum concentration, greatly alleviating the well/barrier-induced high longitudinal resistance. We had a hybrid-mirror VCSEL wafer grown by our subcontractor Lockheed Missiles & Space Company. Its design and reflectance spectrum are presented in Section 4.

New Low-Resistance P-Doped Mirrors

During the contract period, other groups have reported significant improvements in decreasing the resistance of p-type mirrors [Lear, 1992] by smoothly grading the aluminum composition between layers. Even with dopings of 1.5 x 10^{18} cm^{-3}, the current vs. voltage (I/V) characteristics are linear, indicating the absence of well/barrier-induced resistance. Absorption losses are much lower than they are with conventional mirrors doped at 5 x 10^{18} cm^{-3}. The losses are fairly negligible for cavities having a 1% transmission output mirror (appropriate for 3-quantum-well active material), but still somewhat high for a higher-finesse cavity appropriate for SQW active region. The optical efficiencies for these two cases are included in Table 1, which compares a variety of designs, most of them the modulation-doped design.

Continuity of the Three Basic Designs

The three design approaches discussed above are by no means mutually exclusive. They could, in principle, all be combined into a single viable design. Smooth grading of aluminum concentration in the layer interfaces (low-resistance p-mirror) should be used in optimizing the hybrid-mirror design, since for the same resistance, a higher reflectivity could be obtained by utilizing larger differences in aluminum concentration. Modulation doping is utilized in our hybrid-mirror design and should also be used in smoothly-graded p-mirror designs.

Confinement of Current to the Central Portion of the Cavity

A design feature which is independent of the three design approaches discussed above is the importance of confining current flow to the central portion of the VCSEL cavity. Measurements of the optical intensity profile in VCSELs show the $1/e^2$ intensity diameter of the emitted beam to be about 1/2 the diameter of the electrical contact which forms the optical aperture. Thus, most of the optical intensity is in about 1/4 the area of the aperture. Pumping current outside this region produces carriers which are either largely lost to nonradiative recombination, or they help induce higher-order transverse modes which complicate use of the VCSELs in systems. This confinement, and the gaussian intensity profile, are illustrated in Fig. 2b.

Our process follower includes separate photolithographic steps for patterning the deep ion implant (which defines the current flow through the cavity) and the top ohmic contact (which defines the optical aperture). This allows us to confine the current to smaller diameters than the optical aperture as discussed above. Specifically, most of our devices have 5-μm-diameter current flow and 10-μm-diameter ohmic contacts ("5-10" design). This combination is good for low threshold and stable single-transverse-mode output. We also have devices of "7.5-15" design. The optimization of these two diameters is fairly empirical. Thus our photolithographic mask sets include regions for patterning devices with a wide range of diameters of both current flow and ohmic contact. In this way, we can experimentally optimizes these two parameters.

Calculated Performances of VCSEL Designs

In Table 1 we present calculated performances of some of the VCSEL designs discussed above. This table has the same format as the table presented in the proposal, but there are important differences. First, the losses assumed for the n-doped mirror have been reduced from 0.0005 to 0.0001. This reduction is appropriate for advanced VCSEL designs which incorporate modulation doping and/or smoothly-varying aluminum composition in the n-doped bottom mirror. Second, in the multiple-layer modulation-doped structures absorption due to the lightly-doped regions is included. A doping concentration of 1 x 10^{17} cm^{-3} was assumed for these regions, which still produces non-negligible absorption due to their thickness and placement in the intensity peaks of the standing waves. Third, some designs which are not considered for this project have been deleted, while two new ones are included: the smoothly-graded low-resistance p-mirror design and the 8-period modulation-doped structure with maximum doping of 1 x 10^{19} cm^{-3}.

material	thickness	ρ (μΩ-cm)	α (cm-1)	A	η (.990)	η (.998)	Z (Ω)
"old standard" (5E18)	(0.5 μm)	NA	50	.0026	.79	.43	NA
"new p-type" (1.5E18)	(0.5 μm)	NA	10	.00085	.92	.70	
p++(1E20)	500 Å	1,000	500	.00027	.97	.88	16
p++(1E21)	300 Å	333	1,500	.00023	.98	.90	8
p+ (1E19) 4 layers	600 Å each	5,000	100	.00039	.96	.84	16
p+ (1E19) 8 layers	600 Å each	5,000	100	.00068	.94	.75	8
p++(1E20) 4 layers	250 Å each	1,000	500	.00026	.97	.88	8
p++(1E21) 4 layers	150 Å each	333	1,500	.00024	.98	.89	4

Table 1. Calculated values of single-pass absorption A, differential quantum efficiency η for mirror reflectivities 0.99 and 0.998 (appropriate for four- and single-quantum-well active layers, respectively), and p-side spreading resistance Z, for designs incorporating conductive layers of resistivity ρ, and absorptivity α. The "new p-type" design incorporates a p-doped mirror with smoothly-graded interfaces.

3. Process Design

We have developed a detailed Process Follower for the Modulation-Doped Low-Resistance VCSEL as follows. Note: PR = photoresist; ISO = isopropyl alcohol; DI = deionized water

Alignment PR
- Wafer pre-clean (acetone, ISO, DI rinse to 16 MΩ)
- Resist coat AZ1370 (~ 1.2 μm)
- Pre-bake
- Exposure - Alignment Marks Mask
- Chlorobenzene (2.5 minutes)
- Develop
- O_2 descum - (O_2 descum okay since active region is covered by photoresist)
- PR inspection
- ion beam etch (5000 Å) or
  - metalization (Ti = 200 Å, Au = 500 Å)
- photoresist strip in acetone
- wafer clean (ISO, DI rinse)

Active Region Implantation
- Dehydration
- Resist coat - OCG 812 (~6 μm)
- Pre-bake
- Exposure - Active Region Isolation Mask
- Post-Exposure Bake for Image Reversal
- Develop
- O_2 descum
- PR inspection and thickness verification
- Hydrogen implantation (low tilt ~ 5°, rotated, typical 100 keV @ 5e13
- Photoresist strip in acetone
- no descum - unless absolutely required

Device Isolation Implantation (same procedure as active region implant)
- Dehydration
- Resist coat - OCG 812 (~6 μm)
- Pre-bake
- Exposure - Device Isolation Isolation Mask
- Post-Exposure Bake for Image Reversal
- Develop
- O_2 descum
- PR inspection and thickness verification
- Hydrogen implantation (low tilt ~ 5°, rotated, typical 25, 75 keV @ 5e13
- photoresist strip in acetone
- no descum - unless absolutely required

Ohmic Contact Metalization
- Dehydration
- Resist coat (AZ1370, ~ 1.2 μm)
- Pre-bake
- Exposure - Ohmic Metal Mask
- Chlorobenzene (2.5 min.)
- Develop
- O_2 descum
- PR inspection

metallization (Ti = 800 Å, Pt = 1200 Å, Au = 2,000 Å)
photoresist strip in acetone
wafer clean (ISO, DI rinse)

Interconnect Metallization
Dehydration
Resist coat (AZ1375, ~ 1.2 μm)
Pre-bake
Exposure - Interconnect Metal Mask
Chlorobenzene
Develop
O_2 descum
PR inspection
metalization (Ti = 1,000 Å, Au = 7,000 Å)
photoresist strip in acetone
wafer clean (ISO, DI rinse)

Backside Metalization
metalization (AuGe = 1,000 Å, Ni = 150 Å, Au = 2000 Å)
Rapid Thermal Anneal (400°C, 60 sec)

Dielectric Mirror Patterning
Dielectric mirror deposition
wafer clean (ISO, DI rinse)
Dehydration
Resist coat (AZ1375, ~ 1.2 μm)
Pre-bake
Exposure - Dielectric Mirror Mask
Develop
O_2 descum
PR inspection
wet etch (60:10:3 H_2O:H_2SO_4 97%:HF 49%, 6.5 periods/min @ 37°C)
Inspection and mesa thickness
photoresist strip in acetone
wafer clean (ISO, DI rinse)
descum

4. Experimental Results

725 nm VCSELs

We demonstrated an 8x8 array of VCSELs emitting at 725 nm wavelength at room temperature. A photograph of the array, with several elements activated, is shown in Fig. 1. Low film sensitivity at 725 nm greatly reduced the apparent brightness of the VCSELs in the photograph. Thresholds of 21 mA with 100 ns pulses were recorded for 15-μm diameter devices. The design, which avoids current flow through the top mirror, is based on one we recently reported[Jewell, 1992; Scherer, 1992], but with higher aluminum concentrations for emission at the shorter wavelengths. Molecular beam epitaxy (MBE) was used to grow 32 pairs of n-doped $Al_{0.3}Ga_{0.7}As$/GaAs bottom mirror layers, the active region containing 500 Å of $(GaAs)_4(AlAs)_1$ superlattice, and a 1-μm-thick p-doped heterostructure top conductive layer. 11 1/2 pairs of alternating SiO_2/Si_3N_4 layers, deposited by reactive sputtering, formed a high-reflectivity mirror which completed the laser cavity. As previously, individual laser elements were defined by ion milling of mesas through the p-n junction, followed by planarization with SiO_2 to define the

current path. Then, Au-Zn p-contacts were deposited around the mesa tops and alloyed for current injection. Finally, another ion milling step was used to isolate individual contacts.

Light at 720-740 nm is generated by the superlattice active region and the output emits through the annular p-contact. GaAs/AlAs superlattices are reported to be superior to alloy AlGaAs in luminescent efficiency. The p-side resistance is reduced by beryllium modulation-doping in the top of the cavity. In this device the p-conductive region comprised alternating layers of $Al_{0.3}Ga_{0.7}As$ and $Al_{0.5}Ga_{0.5}As$. The heterostructure serves to equalize the current density throughout the microlaser active region, rather than allowing it to crowd preferentially around the outer edges. Furthermore, the lower-Al-concentration layers contained higher Be-doping concentrations and they were centered at the minimum-intensity regions of the standing waves in the optical cavity; thus the maximum absorptivity overlapped the minimum light intensity. Poor adhesion of the SiO_2 insulating layer to the high-aluminum-content sidewalls prevented annealing of the ohmic contacts, thus the current vs. voltage characteristic shows a soft turn-on. The specific resistance is $\sim 2\times10^{-4}\ \Omega cm^2$, or about 2.5 times higher than for our previous low-resistance VCSELs [Jewell, 1992; Scherer, 1992], but still far lower than conventional VCSELs with annealed contacts. The low resistance design allows the devices to handle pulsed currents of over 50 mA through 15-µm diameters ($\sim$25 kA/cm^2). This high-current capability is obviously important for high-power applications.

Since the contact diameter is smaller than that of the pumped region, most of the light intensity is within an area about one-sixth that of the region being pumped. The poor overlap is partly responsible for the low quantum efficiency indicated by the light vs. current plot of Fig. 4. It can be avoided through use of a buried implant having a smaller diameter than the contact, resulting in not only increased quantum efficiency, but single-transverse-mode emission. Other likely causes are current leakage through the active region due to heating caused by the high currents employed, and non-optimized reflectivity in the top mirror.

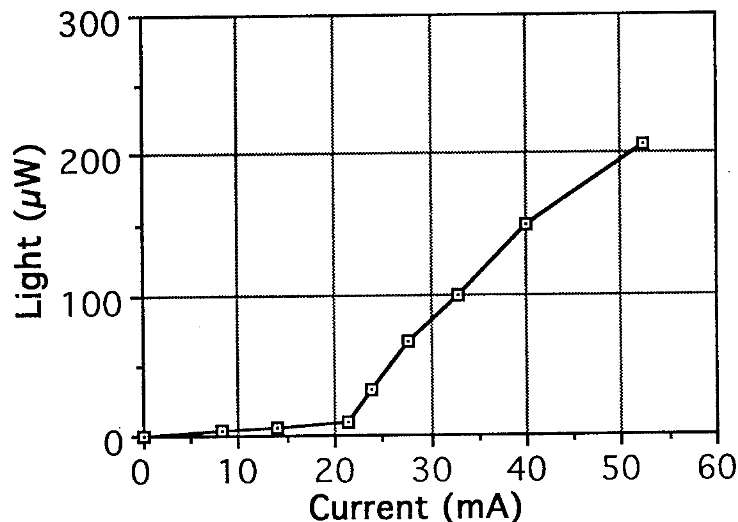

Figure 3. Light vs. current for the 10-µm-diameter, 725-nm-emitting VCSEL.

850 nm Hybrid-Mirror Wafer

We designed, and had grown, a hybrid-mirror VCSEL wafer by Lockheed. Deferment of contract funds delayed the fabrication of this wafer into FY94. We have performed process development to verify key steps in the process follower outlined in Section 3. Etching of the dielectric mirrors is still under development. TiO_2/SiO_2 mirrors, of the kind to be employed in the VCSELs, were deposited on test wafers. This portion of the process development, as well as the wafer processing will take place in PRI's in-house facility early in FY 94. Below we present the design of the wafer and its reflectivity spectrum showing a resonance at ~840 nm.. The portion of the wafer from which the reflectivity spectrum was taken exhibited a photoluminescense peak at about 843 nm, well within the ~10-nm tolerance for matching these the cavity resonance and photoluminescense. Thus the wafer is considered valid for processing.

Device Structure:

Material	X/Y (Al/In)	Thickness (µm)	Density (cm-3)	Type	Dopant
GaAs		0.0030	2 E+19	p	Be
AlGaAs	0.25	0.0504	2 E+19	p	Be
AlGaAs	0.40	0.0150	1 E+19	p	Be
AlGaAs	0.50	0.0030	1 E+19	p	Be
AlGaAs	0.50	0.0436	1 E+18	p	Be
		1 period of the above layers			
AlGaAs	0.50	0.0030	3 E+18	p	Be
AlGaAs	0.40	0.0150	3 E+18	p	Be
AlGaAs	0.25	0.0030	3 E+18	p	Be
AlGaAs	0.25	0.0410	1 E+18	p	Be
AlGaAs	0.25	0.0030	1 E+19	p	Be
AlGaAs	0.40	0.0150	1 E+19	p	Be
AlGaAs	0.50	0.0030	1 E+19	p	Be
AlGaAs	0.50	0.0436	1 E+18	p	Be
		7 periods of the above layers			
AlGaAs	0.50	0.0643	5 E+17	p	Be
AlGaAs	0.25	0.0440	-	U/D	
		1 period of the above layers			
GaAs		0.0090	-	U/D	
AlGaAs	0.25	0.0080	-	U/D	
		3 periods of the above layers			
AlGaAs	0.25	0.0360	-	U/D	
AlGaAs	0.50	0.0590	2 E+18	n	Si
AlAs		0.0711	2 E+18	n	Si
		1 period of the above layers			
AlGaAs	0.25	0.0615	2 E+18	n	Si
AlAs		0.0711	2 E+18	n	Si
		32 periods of the above layers			
GaAs		0.5000	2 E+18	n	Si

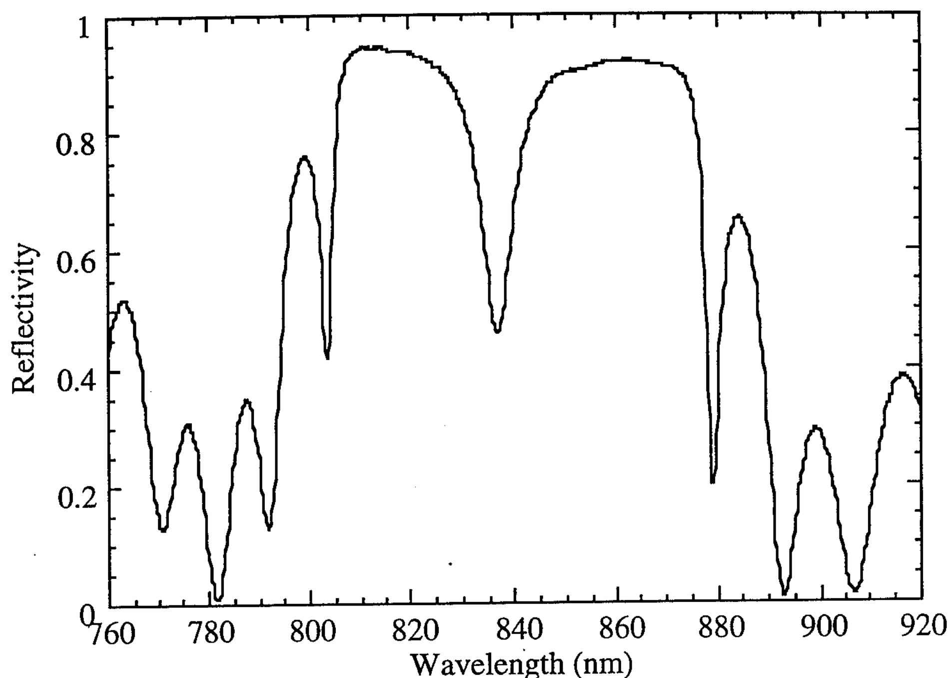

Figure 4. Reflectivity spectrum of the hybrid-mirror VCSEL wafer.

Section 5. Patent Applications

Two U.S. Patent applications have been filed which are related to this contract:

- U.S. Patent Application serial number 07/978,391 "Optical Beam Delivery System," filing date 18 November 1992.
- U.S. Patent Application serial number 07/994,976 "Vertical Cavity Surface-Emitting Laser with Expanded Cavity," filing date 22 December 1992.

More information relating to these patent applications will be provided in the forthcoming Annual Invention Report.

Section 6. Related Publications

J.L. Jewell, A. Scherer, M. Walther, J.P. Harbison, and L.T. Florez, "Low-Voltage-Threshold Microlasers," IEEE Lasers and Electro-Optics Society 1992 Annual Meeting, Boston, MA, Nov. 16-19, pp. 544-545, paper DLTA13.3, (1992).

R.P. Bryan, G.R. Olbright, J.L. Jewell, R.P. Schneider, and S. Swirhun, "Vertical-Cavity Microlaser Smart Pixels," IEEE Lasers and Electro-Optics Society 1992 Annual Meeting, Boston, MA, Nov. 16-19, pp. 596-597, paper EOS/OTA2.5, (1992).

J.L. Jewell, A. Scherer, M. Walther, G.R. Olbright, R.P. Bryan, W.S. Fu, J.P. Harbison, and L.T. Florez, "Vertical Cavity Surface-Emitting Lasers: Lower Resistance, Shorter Wavelength," Conference on Lasers and Electro-Optics, CLEO '93, pp. 134-135, invited paper CTuM1, (1993).

J.L. Jewell, G.R. Olbright, R.P. Bryan and A. Scherer, "Surface-Emitting Lasers Break the Resistance Barrier," Photonics Spectra, p. 216-219, Nov. (1992).

Section 7. Related Business Activities

PRI expanded its operations in 1993 to include optoelectronic materials growth, optoelectronic device fabrication and packaging, and materials/device characterization. PRI's facilities include all equipment necessary for the design, fabrication and validation of optoelectronic device and optical system performance necessary to carry out the remaining contract efforts. PRI is currently the only facility in the world dedicated to the in-house design, fabrication, testing and commercialization of LASE-ARRAYs™ and systems based on LASE-ARRAYs™.

The facilities where the work will be performed meets environmental laws and regulations of federal, state of Colorado and City of Longmont, Colorado Governments for, but not limited to, the following groupings: airborne emissions, waterborne effluents, external radiation levels, outdoor noise, solid and bulk waste disposal practices, and handling and storage of toxic and hazardous materials.

Below is a summary of PRI's facilities, equipment and capabilities:

OVERVIEW

- Building: 12,000 sq. ft: Office, R&D, Manufacturing, Class 10^3 and 10^4 Clean-Rooms
- Optoelectronics Materials Growth Facility
- Optoelectronic Device Fabrication and Packaging Facility
- Optoelectronic Device & Systems Characterization and Testing Facility

FACILITIES & EQUIPMENT

Optoelectronic Materials Growth Facility

Production MBE Growth Reactor
- 3"- Wafer Diameter MBE Wafer System
- RHEED, Quadruple Mass Spectrometer, Flux Measurement, In-situ Thickness Monitor

Optoelectronic Device Fabrication and Packaging Facility

Photolithography
- sub-micron front/back-side Mask Aligner

Metal Deposition
- e-beam Evaporator

Plasma Processing
- Reactive Ion Etching
- Plasma Enhanced Chemical Vapor Deposition

OEIC Processing & Packaging
- Photoresist Spinner & Oven
- Plasma Asher
- Electroplating System
- Optomechanical Assembler
- Wafer Saw & Thinner
- Alloying System
- Wire-Bonder

Optoelectronic Device & Systems Characterization & Testing Facility

Materials/Device Characterization Facilities
- Electro-chemical Profilometer
- Defect Measurement System
- Step-Height Profilometer
- Nomarski Microscope
- Spectrometer/Optical Multichannel Analyzer
- Photoluminescence and Photo-excitation
- Hall Measurement System
- Double crystal X-ray Diffractometer
- Ellipsometer
- Sheet resistivity Measurement System
- High-power UV Inspection
- Reflectance

Device Characterization Facilities
- Automated L-I-V Characterization
- Micro-optic Characterization System
- High-speed Electrical/Optical Measurements
- Probe Station
- Scanning Matrix

CAPABILITIES

PRI supplies commercial custom 2-inch and 3-inch diameter MBE wafers and offers state-of-the-art optoelectronic device fabrication and packaging. Materials, device fabrication and device packaging capabilities include manufacture of: LASE-ARRAYs™ detectors, electro-absorption modulators, serial and parallel laser driver circuits, and micro-optic components.

Optoelectronic & Electronic Materials Growth Capabilities

GaAs/AlGaAs/InGaAs (vertical cavity surface-emitting lasers, heterojunction bipolar transistors [HBT] and phototransistors, field-effect transistors [FET], PIN detectors, metal-semiconductor-metal detectors [MSM], etc.)

Optoelectronic & Electronic Device Fabrication Capabilities

- VCSEL Diodes
- Transistors: HPT, HBT, FET
- Electro-Absorption Modulators
- Parallel/Serial Laser Driver Circuit
- PIN photodiodes
- MSM Detectors
- Microlens Fabrication

Optoelectronic Device Packaging Capabilities

- Wafer Dicing & Sawing
- Wire-bonding
- Flip-Chip Bonding
- High-speed Measurements: Electrical and Optical
- Opto-mechanical Assembly: Micro-Optics Integration

Section 8. References

Bryan, R.P., R.P. Schneider, J.A. Lott, and G.R. Olbright, "Visible InGaP/InAlGaP Strained Quantum-Well Vertical-Cavity Surface-Emitting Lasers," OSA Annual Meeting 1991, post deadline paper PD27 (1991a).

Jewell, J.L., Scherer, A., Walther, M., Harbison, J.P., and Florez, L.T., "Low-Voltage-Threshold Microlasers," Conference on Lasers and Electro-Optics CLEO '92, Optical Society of America, postdeadline paper CPD21 (1992a).

Jewell, J.L. and G.R. Olbright, "Surface-Emitting Lasers Emerge from the Laboratory," Laser Focus World, vol. 28, p. 217, May (1992b).

Jewell, J.L., G.R. Olbright, R.P. Bryan and A. Scherer, "Surface-Emitting Lasers Break the Resistance Barrier," Photonics Spectra, p. 216, Nov. (1992c).

Lear, K.L., Chalmers, S.A., and Killeen, K.P., "A Very Low Voltage and Current Density Threshold Vertical-Cavity Surface-Emitting Laser," IEEE/LEOS Annual Meeting, postdeadline paper PD1, Boston, MA, November 17, 1992.

Olbright G.R., J.L. Jewell and R.P. Bryan "Surface-Emitting Lasers for High-Speed Optical Addressing," NSF SBIR Final Technical Report, Aug (1992d).

Scherer, A., Jewell, J.L., Walther, M., Harbison, J.P., and Florez, L.T., "Fabrication of Low Threshold Voltage Microlasers," Electron. Lett., 28, pp. 1124-1125 (1992).

Schneider, R.P., Bryan, R.P.,, Lott, J.A. and Olbright, G.R., "Visible-Light (657 nm) InGaP/InAlGaP Strained Quantum-well Vertical-Cavity Surface-Emitting Laser," Appl. Phys. Lett., vol. 60, pp. 1830-1832 (1992).

Tell, B., Brown-Goebeler, K.F., Leibenguth, R.E., Baez, F.M., and Lee, Y.H., "Temperature Dependence of GaAs-AlGaAs Vertical Cavity Surface Emitting Lasers," Appl. Phys. Lett., 60, 683 (1992).